© 2017. Published by The Company of Biologists Ltd | Development (2017) 144, 1976-1987 doi:10.1242/dev.148916

RESEARCH ARTICLE

G9a controls placental vascular maturation by activating the Notch Pathway

Lijun Chi[1], Abdalla Ahmed[1,2], Anna R. Roy[1,2], Sandra Vuong[1,2], Lindsay S. Cahill[1,3], Laura Caporiccio[1], John G. Sled[1,3], Isabella Caniggia[4], Michael D. Wilson[2,5,6] and Paul Delgado-Olguin[1,2,6,*]

ABSTRACT

Defective fetoplacental vascular maturation causes intrauterine growth restriction (IUGR). A transcriptional switch initiates placental maturation, during which blood vessels elongate. However, the cellular mechanisms and regulatory pathways involved are unknown. We show that the histone methyltransferase G9a, also known as Ehmt2, activates the Notch pathway to promote placental vascular maturation. Placental vasculature from embryos with G9a-deficient endothelial progenitor cells failed to expand owing to decreased endothelial cell proliferation and increased trophoblast proliferation. Moreover, G9a deficiency altered the transcriptional switch initiating placental maturation and caused downregulation of Notch pathway effectors including *Rbpj*. Importantly, Notch pathway activation in G9a-deficient endothelial progenitors extended embryonic life and rescued placental vascular expansion. Thus, G9a activates the Notch pathway to balance endothelial cell and trophoblast proliferation and coordinates the transcriptional switch controlling placental vascular maturation. Accordingly, *G9A* and *RBPJ* were downregulated in human placentae from IUGR-affected pregnancies, suggesting that G9a is an important regulator in placental diseases caused by defective vascular maturation.

KEY WORDS: G9a, Ehmt2, Vascular maturation, Placental vascular development, Intrauterine growth restriction, Epigenetic regulators, Gene expression, Mouse, Human

INTRODUCTION

The placenta mediates transport between the mother and the fetus through a complex vascular network. Defects in placental vascular development can cause embryonic death and abnormal organogenesis, can negatively affect fetal growth and can confer a higher risk of disease in the postnatal life (Barker et al., 1989). For example, defective patterning of the fetoplacental vasculature, also known as the labyrinth, results in abnormal heart development in mouse (Shaut et al., 2008) and human (Demicheva and Crispi, 2014), and causes intrauterine growth restriction (IUGR) (Barut et al., 2010). IUGR affects up to 32% of pregnancies in some developing countries (Ananth and Vintzileos, 2009), and can cause cardiovascular disease *in utero* and in adulthood (Demicheva and Crispi, 2014). Understanding the mechanisms controlling development of the placental vasculature is essential to uncover the developmental origins of disease.

A key time point during placental development is the transition from a developmental phase to a maturation phase, which occurs at mid gestation (Knox and Baker, 2008). The developmental phase spans from day 32 to month 5 of pregnancy in humans (Benirschke et al., 2012) and from embryonic day (E) 8.5 to E12 in the mouse (Knox and Baker, 2008). During the developmental phase, placental blood vessels branch to create a complex network. After the fifth month of pregnancy in humans, and E12 in mice, the placental vasculature transitions to the maturation phase during which placental blood vessels elongate (Benirschke et al., 2012). In humans, placental vascular elongation requires proliferation and migration of endothelial cells and is accompanied by a concomitant decrease in the proliferation of trophoblasts (Benirschke et al., 2012; Kaufmann et al., 1985), which provide angiogenic signals to the endothelial cells (Adamson et al., 2002; Kaufmann et al., 1985).

The mechanisms controlling blood vessel elongation are not well understood. Evidence *in vitro* and in the mouse retina suggests that modulating the Notch pathway in endothelial cells favors vessel enlargement (Pedrosa et al., 2015; Ubezio et al., 2016). Notch signaling is required for vascular development and remodeling (Roca and Adams, 2007), and the main Notch effector, the transcription factor recombination signal binding protein for immunoglobulin kappa J (Rbpj), is required for extra-embryonic blood vessel maturation (Copeland et al., 2011). The Notch pathway might also be involved in human placental maturation, as the Notch receptor *NOTCH1* and its ligand *JAG2* are downregulated in placentae affected by IUGR (Sahin et al., 2011). However, the mediators controlling the balance between endothelial cell and trophoblast proliferation in the maturing placenta, and the function of the Notch pathway in endothelial cells during vascular maturation are unknown.

The transition from the developmental to maturation phase is accompanied by a transcriptional switch in the expression of ∼700 genes that occurs from E12 to E13.5 (Knox and Baker, 2008). These dramatic gene expression changes imply a role for global transcriptional regulators during the transition. Epigenetic regulators coordinate global gene expression patterns by modifying chromatin structure and controlling the access of transcription factors to their target genes, and also control vascular development (Delgado-Olguin et al., 2014; Griffin et al., 2011). The euchromatic histone-lysine N-methyltransferase (G9a; also known as Ehmt2) can both repress and activate gene expression. G9a mediates gene repression by di-methylating lysine 9 of the histone H3 (H3K9me2), and by scaffolding the interaction of repressor protein complexes at target genes (Shinkai and Tachibana, 2011; Tachibana et al., 2002). In addition, G9a also co-activates gene expression through interaction with histone acetyl transferase complexes (Oh et al., 2014) and

[1]Translational Medicine, The Hospital for Sick Children, Toronto, Ontario M5G 0A4, Canada. [2]Department of Molecular Genetics, University of Toronto, Toronto, Ontario M5S 1A8, Canada. [3]Department of Medical Biophysics, University of Toronto, Toronto, Ontario M5G 1L7, Canada. [4]Lunenfeld-Tanenbaum Research Institute, Mount Sinai Hospital, Toronto, Ontario M5G 1X5, Canada. [5]Program in Genetics & Genome Biology, The Hospital for Sick Children, Toronto, Ontario M5G 0A4, Canada. [6]Heart & Stroke Richard Lewar Centre of Excellence, Toronto, Ontario M5S 3H2, Canada.

*Author for correspondence (paul.delgadoolguin@sickkids.ca)

Received 11 January 2017; Accepted 13 April 2017

Development (2017) 144, 1976-1987 doi:10.1242/dev.148916

estrogen receptors (Purcell et al., 2011). G9a is required for embryonic development. Constitutive *G9a* mutant mice die at E12.5 (Tachibana et al., 2002), and fail to inactivate some imprinted genes in placental trophoblasts at E9.5, but appear to develop a normal placenta at this stage (Nagano et al., 2008; Wagschal et al., 2008). Thus, G9a is not required for early placental development up to E9.5. However, the function of G9a in specific placental cell types in later aspects of placental vascular development, such as vascular maturation, or in placental disease is unknown.

RESULTS

G9a in endothelial progenitors and their derivatives is required for embryonic survival and organogenesis

To uncover the function of G9a in vascular development, we inactivated *G9a* in endothelial progenitors and their derivatives by Tie2-Cre-mediated homologous recombination of a conditional allele (Proctor et al., 2005). G9a was efficiently inactivated as shown by decreased G9a and H3K9me2 in embryo body and placental endothelial cells in E10.5 *G9a* mutant embryos (Fig. S1). Thus, G9a is the major H3K9me2 methyltransferase in embryonic endothelial cells.

G9a is dispensable for endothelial cell specification because expression of the endothelial marker Pecam1 and of GFP driven by a Tie2-Cre-activated $Rosa^{mT/mG}$ reporter transgene (Muzumdar et al., 2007) revealed a normal vascular pattern in E9.5 *G9a* mutant embryos (Fig. S2). *G9a* heterozygotes were recovered at the expected ratios and grew to adulthood. In contrast, *G9a* homozygous mutants died by E16.5 (Table S1), indicating that G9a is essential for vascular development.

G9a mutant embryos appeared normal at E10.5, but became pale starting at E13.5. Endothelial cells are essential for liver development (Lammert et al., 2003); accordingly, *G9a* mutants had an underdeveloped liver (Fig. S3).

Knockout of G9a-like protein (GLP; also known as Ehmt1) concomitant with knockdown of G9a in cardiovascular progenitor cells has been shown to cause cardiac septation defects (Inagawa et al., 2013). In our experiments, G9a was inactivated in endocardial cushions (ECs) (Fig. S4A-D), which fuse to form the membranous cardiac septum. Apoptotic EC cells positive for activated caspase 3 were increased in *G9a* mutants (Fig. S4E-G). Accordingly, interventricular septation was incomplete in mutant hearts (Fig. S4H-K), indicating that G9a is required in ECs for interventricular septation. Thus, G9a is required for development of endothelial derivatives in specific organs, including the liver and heart.

G9a is required for expansion of the placental labyrinth

Analysis of the umbilical cord revealed stenosis of the umbilical artery in *G9a* mutant E13.5 embryos (Fig. S5), suggesting a possible function of G9a in placental vascular development. Measurements of control whole placentae showed that the thickness of the capillary-irrigated portion of the normal labyrinth progressively increases from E12.5 to E15.5. The thickness of this area of the labyrinth was comparable between wild-type controls and *G9a* mutant placentae at E12.5; however, *G9a* mutant placentae failed to expand the capillary-irrigated area from this point onwards (Fig. 1A,B). Similarly, quantification on histological sections revealed that the entire labyrinth surface area was comparable between controls and *G9a* mutants at E12.5, but significantly decreased in *G9a* mutants at E13.5 and E15.5 (Fig. 1C,D).

To visualize endothelial cells, we incorporated the $Rosa^{mT/mG}$ transgene (Muzumdar et al., 2007) in mice carrying the conditional allele of *G9a* and expressing *Tie2-Cre*. GFP fluorescence revealed a smaller labyrinth (Fig. 1E), and fluorescence activated cell sorting (FACS) recovered a smaller percentage of GFP^+ cells from *G9a* mutant placentae (Fig. 1F,G). Thus, deficiency of G9a leads to decreased numbers of endothelial cells and decreased labyrinth expansion at E13.5.

G9a is required for structuring the placental labyrinth

To analyze the labyrinth structure in detail, we perfused the placental arterial vasculature in E15.5 control and *G9a* viable mutants with an X-ray contrast agent and scanned them using microcomputed tomography (microCT) (Rennie et al., 2011). We analyzed three-dimensional renderings to quantify the span and depth of the labyrinth, vessel curvature, the number of branching generations, and the diameter of the Strahler order vessels (Rennie et al., 2011, 2015). There was a trend towards a decreased labyrinth span in mutants (mean 6.3±0.4 mm) compared with controls (6.6 ±0.2) (P<0.08). In agreement with measurements on tissue sections (Fig. 1A), *G9a* mutant placentae had a significantly decreased labyrinth depth (mean 1.40±0.12 mm) compared with controls (mean 1.71±0.20 mm) (P<0.02) (Fig. 2A,B).

Large vessels of the labyrinth in the mutant group exhibited marked curvature on surface renderings (Fig. 2C, red line). This feature was not observed in control placentae. Accordingly, the median tortuosity ratio was slightly increased in mutants (mean 1.79±0.56) compared with controls (mean 1.62±0.47) ($P<2\times10^{-16}$) (Fig. 2D).

Although there was no significant difference in the total number of vessel segments in the arterial tree between groups (mean 3927 ±1574 and 2858±1435 for mutants and controls, respectively), there was a trend towards decreased numbers of larger diameter (>200 µm) vessels, and increased numbers of smaller diameter vessels in mutants compared with controls (P<0.08) (Fig. 2E). Analysis of branching structure of the vascular tree with a Strahler ordering scheme revealed that most of the trees had seven orders (two mutants and one control had eight orders). There was no difference in the number of the order 1-7 vessels between the groups. However, there was a significant decrease in the diameters of the Strahler order vessels in mutants compared with controls (P=0.006, two-way ANOVA). Furthermore, there was a significant interaction between Strahler order and group (P=0.02, two-way ANOVA), with the largest difference in diameters on Strahler order 3 vessels (P<0.001) (Fig. 2E,F). Thus, G9a is essential for vessel elongation and maturation, and labyrinth expansion.

Defective migration of G9a-deficient endothelial cells

To uncover the cellular mechanism controlled by G9a required for labyrinth expansion, we analyzed the capacity of *G9a* mutant endothelial cells to establish tight junctions, and their cell shape and migratory capacity. Control and *G9a* mutant cells established tight junctions in confluent cultures, as revealed by membrane localization of zonula occludens-1 (ZO1; also known as Tjp1) (Fig. 3A). Transmission electron microscopy (TEM) showed smaller nuclei in *G9a* mutant than in control endothelial cells (Fig. 3B,C). Endothelial cell shape and nuclear shape are coordinated (Versaevel et al., 2012). To assess cell shape, GFP^+ placental endothelial cells sorted from E12.5 control and *G9a* mutant embryos carrying the $Rosa^{mT/mG}$ transgene were cultured at low confluence on gelatin. *G9a* mutant cells developed shorter filopodia, and were overall shorter than control cells after 72 h in culture (Fig. 3D,E) suggesting that *G9a* mutant cells are less sensitive to migratory stimuli. To assess migratory capacity, we seeded an equal number of control and *G9a* mutant placental endothelial cells and performed migration scratch assays. Fewer

Development (2017) 144, 1976-1987 doi:10.1242/dev.148916

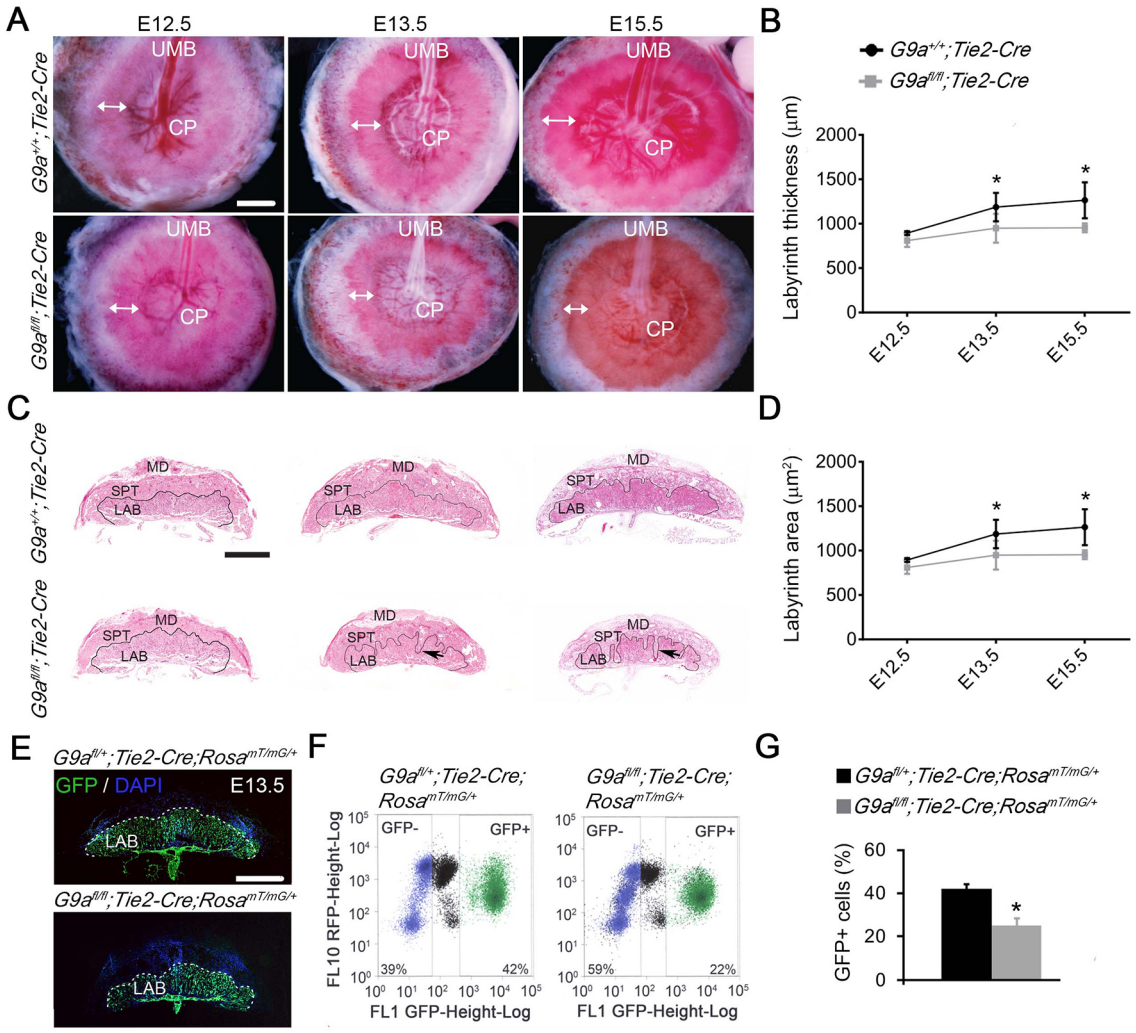

Fig. 1. G9a is required for proper expansion of the placental vasculature. (A) View of the embryonic side of the placenta of control (*G9a*$^{+/+}$*;Tie2-Cre*) and mutant (*G9a*$^{fl/fl}$*;Tie2-Cre*) embryos at E12.5, E13.5 and E15.5. Double arrows indicate the edges of the capillary-irrigated area of the labyrinth. CP, chorionic plate; UMB, umbilical cord. (B) Quantification of the capillary-irrigated area of the labyrinth (*n*=3 placentae per genotype). (C) Hematoxylin and Eosin (H&E)-stained histological sections of placentae. The labyrinth (LAB) is outlined. MD, maternal decidua; SPT, spongiotrophoblast. Arrows indicate invaginations of spongiotrophoblast into the labyrinth. (D) Quantification of the labyrinth area. Plots represent the mean±s.d. of three placentae per genotype. (E) Sections of placentae from control (*G9a*$^{fl/+}$*;Tie2-Cre;Rosa*$^{mT/mG/+}$) and mutant (*G9a*$^{fl/fl}$*;Tie2-Cre,Rosa*$^{mT/mG/+}$) embryos carrying the *Rosa*$^{mT/mG}$ transgene, which labels the labyrinth with GFP. Nuclei were counterstained with DAPI. Dashed line delineates the edge of the labyrinth. (F) Representative FACS plots of labyrinth cells showing the percentage of GFP negative and positive cells. (G) Quantification of the percentage of GFP-positive cells. Data represent the mean±s.d. of sorting analyses on five placentae per genotype. **P*<0.05. Scale bars: 1 mm.

G9a mutant cells migrated into the scratched zone compared with controls (Fig. 3F,G), indicating decreased migratory capacity. Thus, decreased migratory capacity of *G9a* mutant endothelial cells might contribute to defective placental vascular maturation.

G9a controls the balance of endothelial and trophoblast proliferation in the placenta

Histological sections showed wedges of spongiotrophoblast invading the labyrinth in *G9a* mutant placentae at E13.5 and E15.5 (Fig. 1C, arrows). To visualize the spongiotrophoblast, we performed *in situ* hybridization for trophoblast specific protein alpha (*Tpbpa*). Quantification on stained sections revealed that the spongiotrophoblast in normal placentae, unlike the labyrinth, which grows progressively from E12.5 to E15.5 (Fig. 1C,D), grows only marginally between these stages (Fig. 4A,B). In contrast, the spongiotrophoblast grows progressively from E12.5 to E15.5 in *G9a* mutant placentae (Fig. 4A,B). Spongiotrophoblast overgrowth as a result of inactivation of *G9a* in labyrinth endothelium suggests that growth of these placental cell types must be coordinated. We quantified proliferating endothelial cells and spongiotrophoblasts in E11.5 to E15.5 control placentae. Endothelial cells were identified by immunofluorescence for GFP in mice carrying the *Rosa*$^{mT/mG}$ and *Tie2-cre* transgenes. Spongiotrophoblasts were identified by immunofluorescence for Tpbpa. Immunofluorescence for GFP and phosphorylated histone H3 showed that endothelial cells increase their proliferation from 31% at E11.5 to 39% at E12.5, and then gradually decrease to 9% at E15.5. In contrast, only 12% and 13.5% of endothelial cells proliferate at E11.5 and E12.5, respectively, and decrease down to 2% at E15.5 in *G9a* mutant placentae (Fig. 4C,D).

Few proliferating spongiotrophoblasts were present in control placentae (Fig. 4E); therefore, we obtained total numbers of proliferating trophoblasts in sections of normal placentae. This analysis revealed an increase of 20% (five to seven cells) from E11.5 to E12.5, and a decrease of 52% (seven to four cells) from E12.5 to

Development (2017) 144, 1976-1987 doi:10.1242/dev.148916

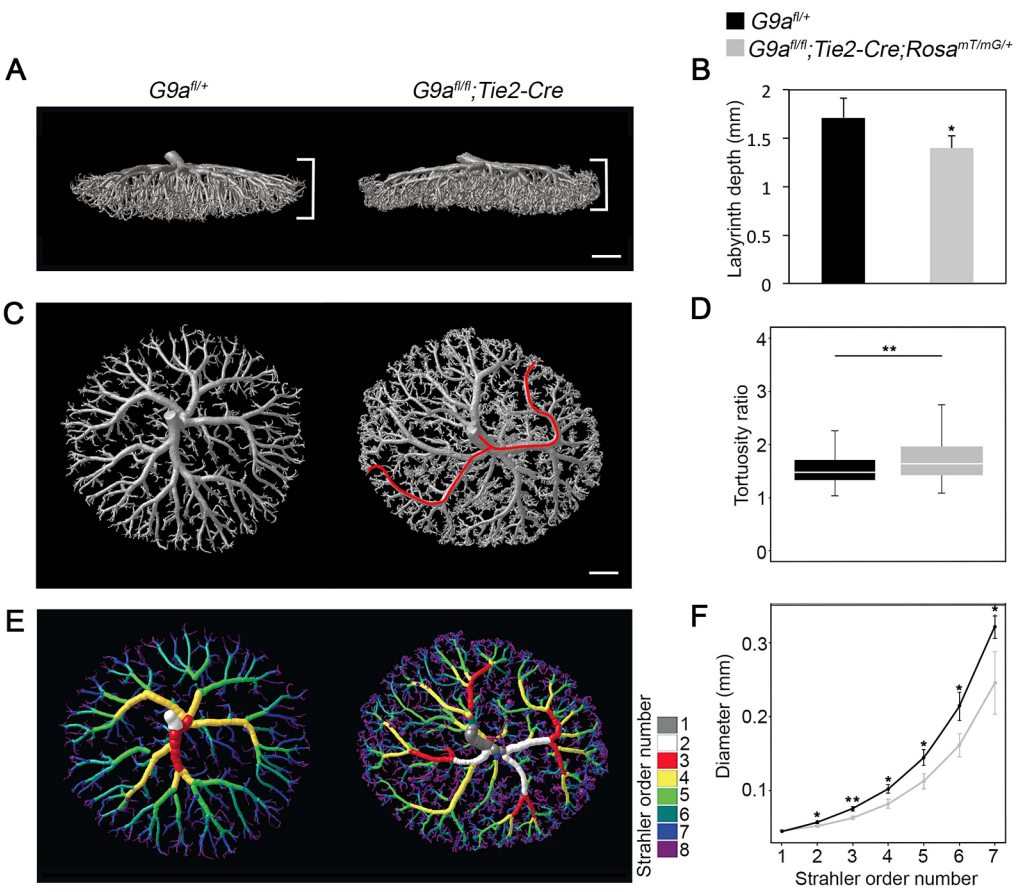

Fig. 2. G9a is required for structuring the placental labyrinth. (A) Surface renderings of control (*G9a*$^{fl/+}$) (n=7) and mutant (*G9a*$^{fl/fl}$;*Tie2-Cre*) (n=4) placentae. Lateral views of the labyrinth. Brackets indicate depth of labyrinth. (B) The labyrinth depth is decreased in mutants (*P<0.02). (C) Increased tortuosity of large vessels was observed in mutants (red line in mutant surface rendering). (D) Box-and-whiskers plot showing an increased vessel tortuosity ratio in mutants compared with controls. (E) Rendering with color-coded Strahler order vessels. (F) The average diameter (shown on a logarithmic scale) of Strahler order 1-7 vessels in control and mutant placentae. There was a significant decrease in the diameters of the Strahler order vessels in the mutants compared with controls. Data shown as mean±s.e.m. *P<0.1; **P<2×10^{-16}. Scale bars: 1 mm.

E13.5. Proliferating trophoblasts then decreased by 82% (one cell from five at E11.5) by E15.5. *G9a* mutant placentae showed significant increases over control placentae of proliferating trophoblasts at E11.5, E12.5, E13.5, E14.5 and E15.5 (Fig. 4E,F). Thus, a significantly higher proportion of endothelial cells versus spongiotrophoblasts proliferate during the normal development-to-maturation transition, and G9a in placental endothelial cells is required to maintain this balance. Thus, decreased endothelial cell migration and proliferation, combined with increased trophoblast proliferation affect placental vascular maturation in the *G9a* mutant placenta.

G9a controls the transcriptional switch from development to maturation in the placental vasculature

To uncover the transcriptional pathways regulated by G9a that control placental vascular development, we analyzed the global gene expression profile in the labyrinth of control and *G9a* mutant placentae at E12 and E13.5, before and after the transition to maturation, respectively, by high-throughput sequencing of RNA. Similar to a previous report (Knox and Baker, 2008), our analysis revealed a transcriptional switch from E12.5 to E13.5. The expression of 3722 genes changed more than 1.5-fold (P<0.05) in normal placentae from E12.5 to E13.5; 1930 genes were down- and 1792 upregulated (Fig. 5A). Analysis of the genes that changed their expression using DAVID (Huang et al., 2009) identified pathways that regulate vascular development and cell proliferation. The top ten pathways associated with upregulated genes include cell adhesion, cell cycle, insulin resistance, and the Notch pathway. The top ten pathways associated with downregulated genes include cytokine-cytokine receptor interaction, TNF signaling, chemokine signaling, and p53 signaling (Fig. 5B). Finely tuned regulation of the Notch pathway is required for vascular maturation (Pedrosa et al., 2015; Ubezio et al., 2016). In addition, expression of the main effector of the Notch pathway, *Rbpj*, in developing endothelial cells is required for vascular maturation in extra-embryonic tissues (Copeland et al., 2011). Most genes in the Notch pathway identified in our analysis were downregulated after the development-to-maturation transition at E13.5. However, the Notch pathway effectors *Rbpj* and mastermind like transcriptional co-activator 2 (*Maml2*), were upregulated (Fig. 5C). Hence, despite downregulation of many Notch ligands and receptors, the activity of Notch effectors might increase during maturation of the normal placenta.

Only 2565 genes changed their expression during the transition to maturation in the *G9a* mutant labyrinth, from which only 1768 overlapped with genes for which expression changed in the control placentae (Fig. 5D). Consistent with the *G9a* mutant labyrinth phenotype, positive regulators of endothelial cell migration and proliferation, including TAL BHLH transcription factor 1 (*Tal1*) (Lazrak et al., 2004), mouse double minute 2 homolog (*Mdm2*) (Secchiero et al., 2007) and glutathione peroxidase 1 (*Gpx1*) (Galasso et al., 2006), were decreased in the *G9a* mutant labyrinth. Thus, G9a controls the transcriptional switch from the development phase to the maturation phase. We used gene set enrichment analysis (GSEA) (Subramanian et al., 2005) to identify pathways associated with genes that were misregulated in the *G9a* mutant labyrinth at E12.5 and E13.5. Interestingly, the analysis identified Notch amongst the most enriched pathway in upregulated genes at E12.5 and E13.5 (Fig. 5E). Accordingly, several Notch receptors and ligands were upregulated in *G9a* mutant labyrinth. However, the Notch effectors *Rbpj* and *Maml2*, which were upregulated during the developmental-to-maturation transition in the normal

Development (2017) 144, 1976-1987 doi:10.1242/dev.148916

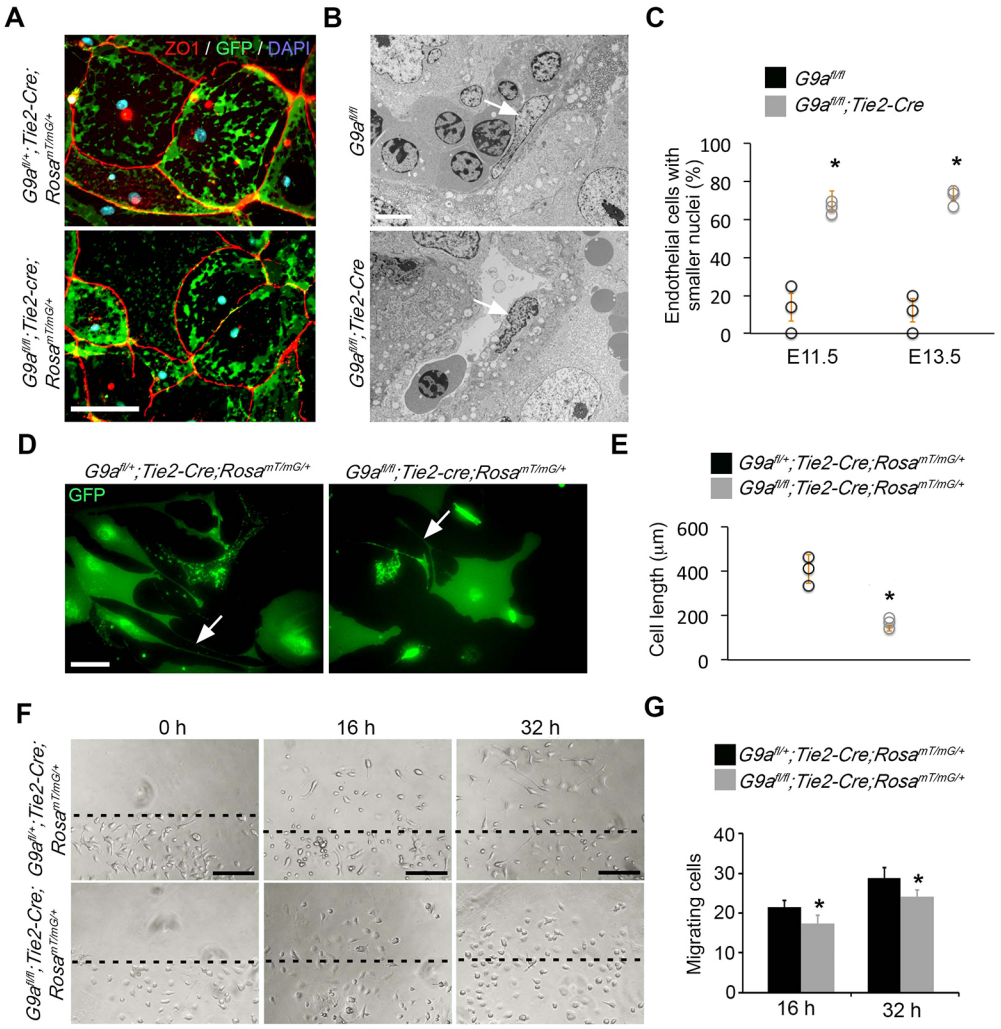

Fig. 3. Defective migration of *G9a*-deficient endothelial cells.
(A) Immunofluorescence of zonula occludens-1 (ZO1) and GFP in endothelial cells isolated from control (*G9a*$^{fl/+}$*;Tie2-Cre;Rosa*$^{mTlmG/+}$) and mutant (*G9a*$^{fl/fl}$*;Tie2-Cre,Rosa*$^{mTlmG/+}$) placentae at E12.5. Nuclei were counterstained with DAPI. (B) TEM on control (*G9a*$^{fl/fl}$) and *G9a* mutant (*G9a*$^{fl/fl}$*;Tie2-Cre*) placental vessels. Arrows point to endothelial cell nuclei. (C) TEM revealed a higher percentage of mutant endothelial cells with reduced nucleus length in placentae at E11.5 and E13.5 (*n*=3). (D) Endothelial cells expressing GFP isolated from control and mutant placentae at E12.5 in low confluence cultures. Arrows point to filopodia, which are shorter in *G9a* mutant cells. (E) Quantification of the total length of endothelial cells isolated from control (*n*=4) and mutant (*n*=4) placentae. (F) Migration scratch assay on control and mutant endothelial cells. The dashed line indicates the edge of the scratch. Cultures were imaged 0 h, 16 h and 32 h after scratching. (G) Quantification of control and *G9a* mutant endothelial cells that migrated into the scratched area after 16 h and 32 h. Data represent the mean±s.d. of six independent experiments. **P*<0.05. Scale bars: 200 µm (A,D,F); 1 µm (B).

labyrinth (Fig. 5C), were decreased in the *G9a* mutant labyrinth (Fig. 5F). Analysis of the 5′ regulatory region of genes downregulated in E12.5 *G9a* mutant labyrinth using Enrichr (Kuleshov et al., 2016) revealed enrichment of RBPJ binding motifs (data not shown), suggesting that the Notch pathway might activate genes important for placental vascular maturation. Western blot analysis confirmed decreased Rbpj levels, and revealed a slight decrease of the cleaved, but not full-length, Notch1, and of Notch2 proteins in *G9a* mutant labyrinth (Fig. 5G,H). This analysis was carried out on labyrinth tissue; therefore, it could have underestimated protein decrease in endothelial cells. *In situ* hybridization (Fig. 5I) confirmed downregulation of *Rbpj* mRNA in *G9a* mutant placental labyrinth. Upregulation of *Rbpj* during normal placental maturation and its downregulation in *G9a* mutant placental endothelial cells was confirmed by qPCR on GFP^{+} cells sorted from the labyrinth of *G9a* mutant embryos carrying the *Tie2-Cre* and *Rosa*$^{mT/mG}$ transgenes (Fig. 5J; Fig. S6). Thus, G9a controls the transcriptional switch from development to maturation and is required for activation of the Notch pathway to promote maturation of the placental vasculature.

G9a controls placental vascular maturation by activating the Notch pathway

Forcing Notch activation in endothelial cells should improve placental vascular maturation in *G9a* mutants. To test this hypothesis, we integrated the *Rosa*^{Notch} transgene into *G9a* mutants. *Rosa*^{Notch} contains a Lox-STOP-Lox cassette between the coding sequence of the intracellular portion of the *Notch1* receptor and the *GT(ROSA)26Sor* promoter. Cre-mediated recombination constitutively activates the Notch1 receptor (Murtaugh et al., 2003). We crossed *G9a*$^{fl/+}$*;Tie2-Cre* males with *G9a*$^{fl/fl}$*;Rosa*$^{Notch/+}$ females, to activate the Notch pathway in *G9a* mutant endothelial progenitor cells. Activation of Notch in control *G9a* heterozygotes did not affect placental morphology (Fig. S7). Only two out of 41 *G9a* live (with beating hearts) mutant embryos were recovered at E16.5 (4% rather than the expected 12.5%), whereas seven out of 41 live *G9a* mutants carrying *Rosa*^{Notch} were recovered at E16.5 (17% rather than the expected 12.5%) (Table S2). Survival curves for *G9a* mutants positive and negative for the *Rosa*^{Notch} transgene analyzed using the Kaplan–Meier method coupled with Gehan–Breslow–Wilcox test revealed that the increase was significant (P<0.01) (Fig. S8). Furthermore, the placental phenotype was rescued in *G9a* mutants carrying the *Rosa*^{Notch} transgene. The labyrinth surface area was normalized in *G9a* mutants expressing the *Rosa*^{Notch} transgene (Fig. 6A-D). In addition, activation of the Notch pathway in *G9a* mutants blunted abnormal trophoblast expansion (Fig. 6E,F). Notch activation did not rescue liver underdevelopment and anemia (Fig. S2B,C), suggesting that defective placental vascular development in *G9a* mutants is not secondary to anemia. Viable *G9a* mutants carrying the *Rosa*^{Notch} transgene were not recovered after E16.5, suggesting that G9a is

Development (2017) 144, 1976-1987 doi:10.1242/dev.148916

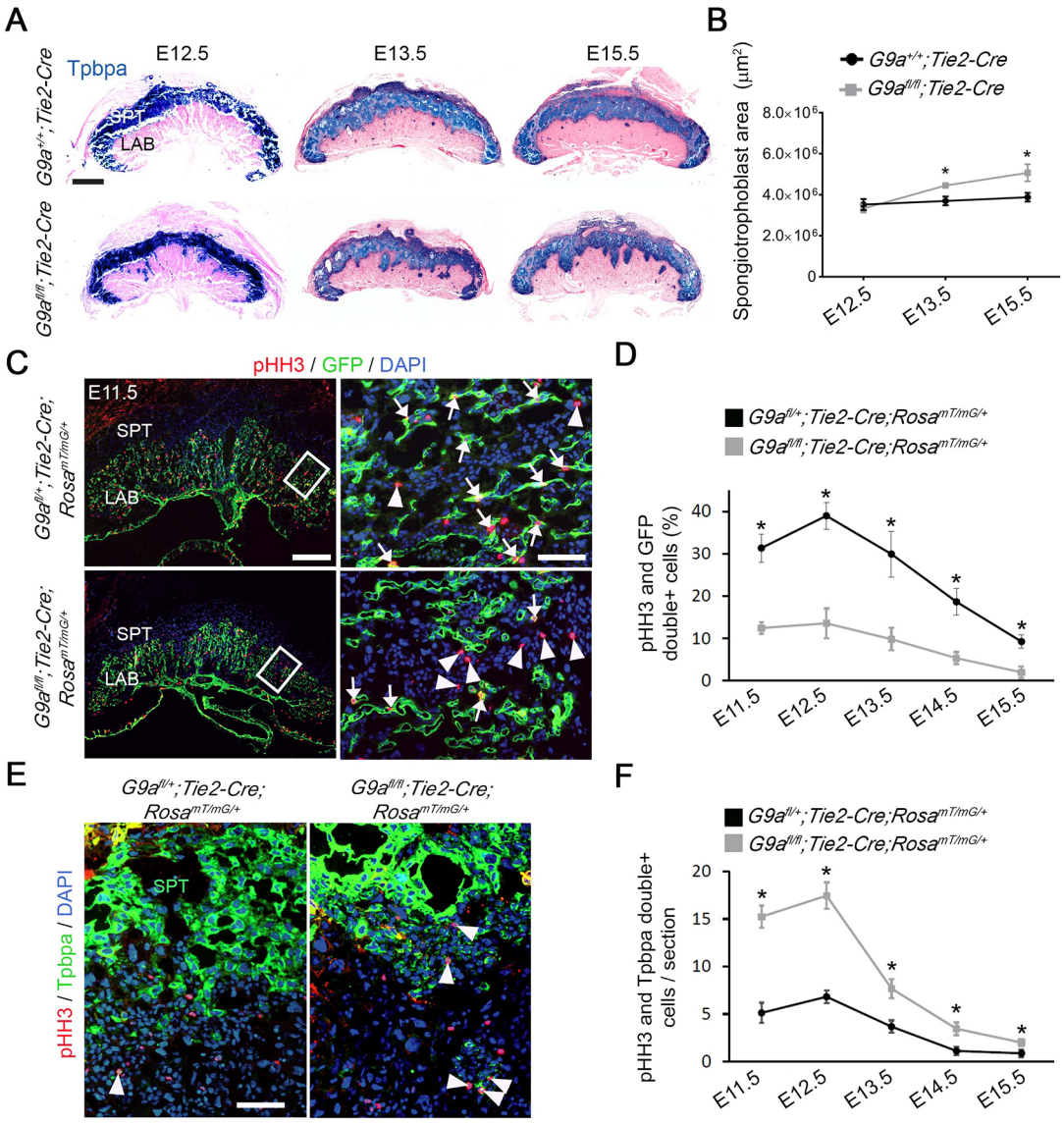

Fig. 4. G9a controls the balance of endothelial and trophoblast proliferation in the placenta. (A) *In situ* hybridization for *Tpbpa* in control (*G9a*$^{+/+}$*;Tie2-Cre*) and mutant (*G9a*$^{fl/fl}$*;Tie2-Cre*) placentae at E12.5, E13.5 an E15.5. (B) Quantification of the spongiotrophoblast (SPT) area. (C) Immunofluorescence for phosphorylated histone H3 (pHH3) and GFP, revealing labyrinth (LAB) endothelium in control (*G9a*$^{fl/+}$*;Tie2-Cre;Rosa*$^{mT/mG/+}$) and mutant (*G9a*$^{fl/fl}$*;Tie2-Cre, Rosa*$^{mT/mG/+}$) placentae at E11.5. Nuclei were counterstained with DAPI. Boxed areas are amplified in right-hand panels. Arrows point to proliferating endothelial cells. Arrowheads point to proliferating GFP^{-} cells. (D) Quantification of pHH3 and GFP double-positive cells. (E) Immunofluorescence for pHH3 and Tpbpa, which reveals spongiotrophoblast (SPT). Arrowheads point to proliferating spongiotrophoblasts. (F) Quantification of Tpbpa and pHH3 double-positive cells. Data represent the mean±s.d. of three placentae per genotype. *P<0.05. Scale bars: 1 mm (A); 500 µm (C,E).

required in non-placental endothelial precursors and their descendants for embryonic survival. Alternatively, G9a might regulate additional placental endothelial functions not assessed in our study. Thus, G9a controls placental vascular maturation by activating the Notch pathway.

G9A and genes in the Notch pathway are downregulated in human placentae affected by IUGR

Our results open the possibility that G9A-mediated modulation of the Notch pathway might be required in human placental maturation and involved in placental diseases such as IUGR. We determined the presence of *G9A* mRNA and protein in the human placenta. *In situ* hybridization and immunohistochemistry revealed G9A in endothelial cells in placental blood vessels of the chorionic plate (Fig. 7A,B). To assess the potential involvement of G9A and the Notch pathway in human placental vascular maturation, we quantified the expression of *G9A* and *RBPJ* in chorionic villi of human placentae affected by IUGR using qPCR. *G9A* and *RBPJ* mRNA and protein, as well as the cleaved but not the full-length NOTCH1 and NOTCH2, were slightly decreased in placentae from pregnancies affected by IUGR (Fig. 7C-E). Our analysis was carried out on placental tissue and thus could have underestimated cell-specific decreases in Notch regulators. Altogether, our results suggest that G9A is a key regulator of placental vascular maturation potentially implicated in human placental disease.

DISCUSSION

Vascular elongation during placental maturation requires proliferation of endothelial cells (Benirschke et al., 2012) and concomitant rearrangement of the surrounding trophoblast. Such

Development (2017) 144, 1976-1987 doi:10.1242/dev.148916

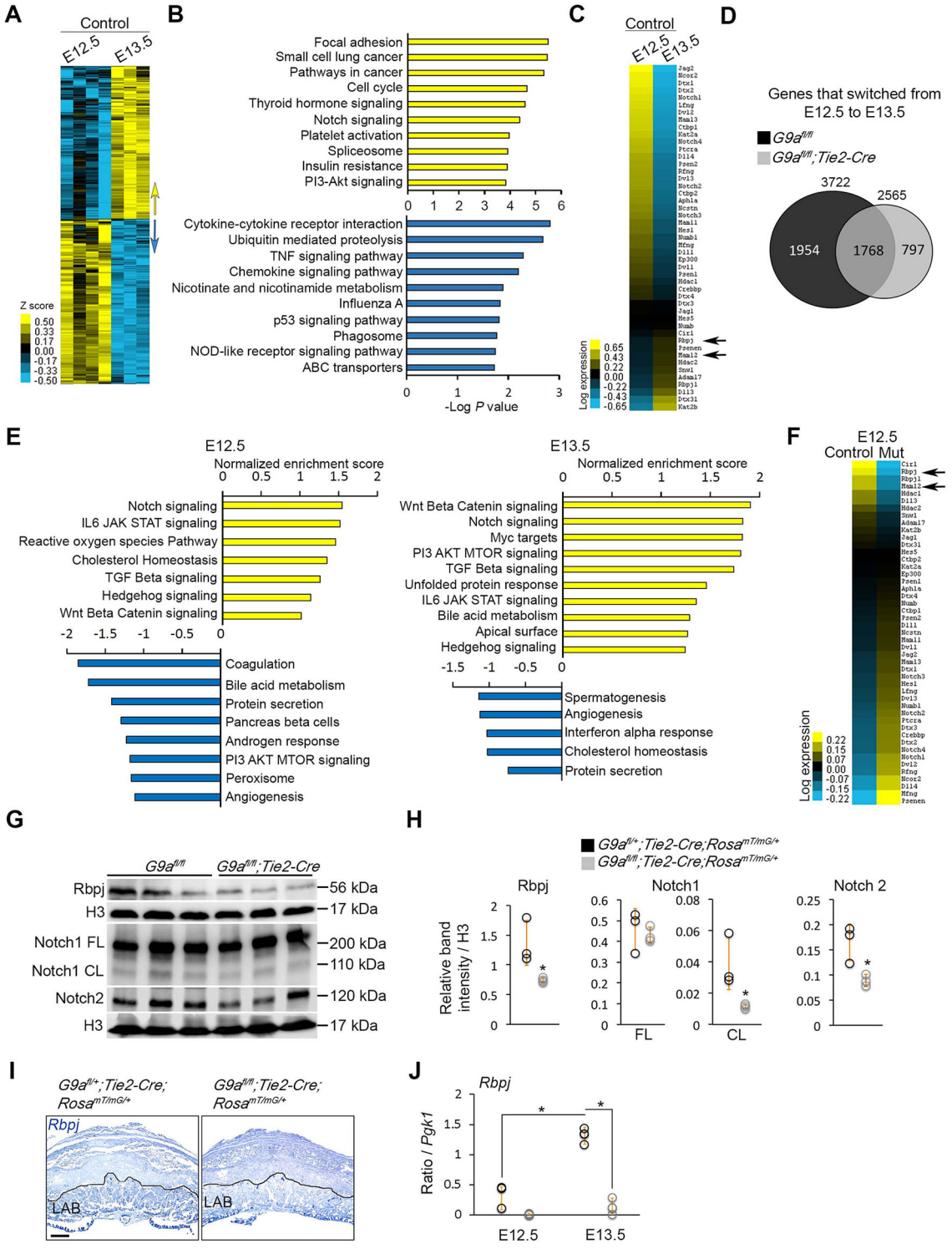

Fig. 5. G9a controls the transcriptional switch during the transition from development to maturation in the placental vasculature. (A) Heat map of differentially expressed genes (P<0.05, fold change >1.5) in labyrinth of control (*G9a*$^{fl/fl}$) placentae at E12.5 (n=4) and E13.5 (n=4). Upregulated genes are in yellow, and downregulated genes in blue. (B) Plots of functional categories with enriched up- and downregulated genes during normal placental vascular maturation. Upregulated pathways are in yellow, and downregulated pathways are in blue. (C) Heat map of log expression levels of genes in the Notch pathway differentially expressed during normal placental vascular development. The Notch effectors *Rbpj* and *Maml2* (arrows) were upregulated in E13.5 labyrinth. (D) Venn diagram of genes misregulated in control (*G9a*$^{fl/fl}$) (n=4) and mutant (n=4) (*G9a*$^{fl/fl}$*;Tie2-Cre*) (n=4) E12.5 and E13.5 labyrinth. (E) Plots of pathways with enriched up (yellow) and downregulated (blue) genes in *G9a* mutant labyrinth at E12.5 and E13.5. (F) Heat map of log expression of genes in the Notch pathway in E12.5 control and *G9a* mutant labyrinth. *Rbpj* and *Maml2* (arrows) were downregulated (blue). (G) Western blot of Rbpj, full length (FL) and cleaved (CL) Notch1, and Notch2 in control and mutant labyrinth at E12.5. Histone H3 was used as loading control. (H) Quantification of band intensity relative to H3 of the blots shown in G. (I) *In situ* hybridization of *Rbpj* in control and *G9a* mutant placentae at E12.5. LAB, labyrinth. Scale bar: 1 mm. (J) qPCR of *Rbpj* in endothelial cells sorted from control (*G9a*$^{fl/+}$*;Tie2-Cre;ROSA*$^{mT/mG}$) and mutant (*G9a*$^{fl/fl}$*;Tie2-Cre;ROSA*$^{mT/mG}$) labyrinth at E12.5 and E13.5. Data represent the mean±s.d. of three placentae per genotype. *P<0.05.

Development (2017) 144, 1976-1987 doi:10.1242/dev.148916

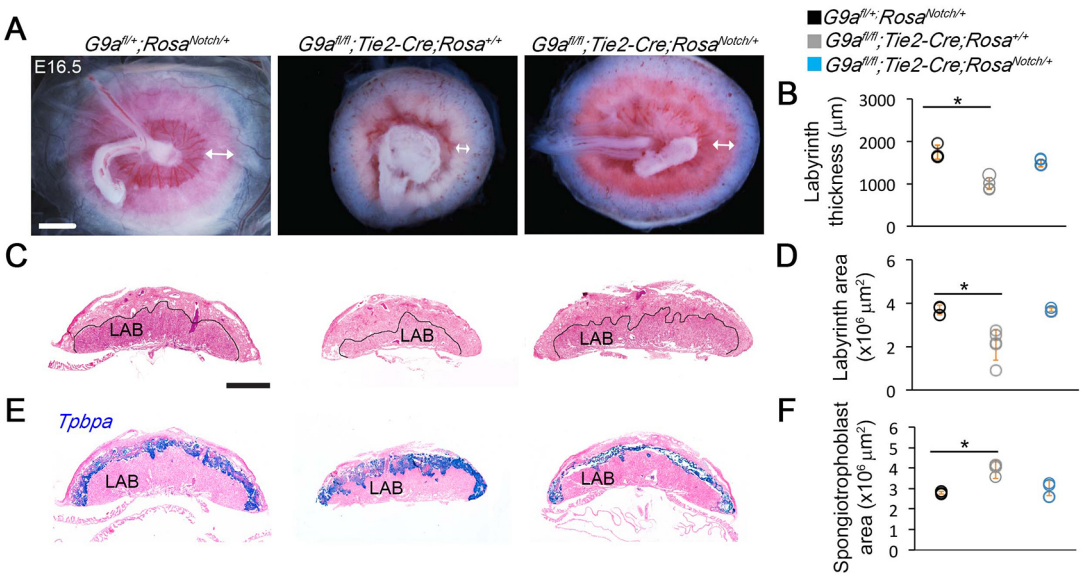

Fig. 6. G9a controls placental vascular maturation by activating the Notch pathway. (A) Placentae of E16.5 control (*G9a*$^{fl/+}$;*Rosa*$^{Notch/+}$), *G9a* mutant (*G9a*$^{fl/fl}$;*Tie2-Cre;Rosa*$^{+/+}$), and *G9a* mutant embryos carrying the *Rosa*^{Notch} transgene (*G9a*$^{fl/fl}$;*Tie2-Cre;Rosa*$^{Notch/+}$). Double arrows indicate the edges of the capillary-irrigated area of the labyrinth. (B) Quantification of the thickness of the capillary-irrigated area of the labyrinth. Data represent the mean±s.d. of three placentae per genotype. *P<0.05. (C) Placental sections stained with H&E. Black line delineates the edge of the labyrinth (LAB). (D) Quantification of the labyrinth surface area. (E) *In situ* hybridization of *Tpbpa*. (F) Quantification of *Tpbpa*-stained spongiotrophoblast surface area. Data represent the mean±s.d. of three placentae per genotype. *P<0.05. The differences between control versus *G9a*$^{fl/fl}$;*Tie2-Cre;Rosa*$^{Notch/+}$ were not significant, P=0.2. Scale bars: 1 mm.

rearrangement is accompanied by reduced proliferation of the trophoblast along the entire length of the elongating vessel (Benirschke et al., 2012). The cellular and molecular events controlling maturation of the placental vasculature are poorly understood in large part because this process has not been systematically investigated in mouse models. We found that mouse endothelial cells actively proliferate, whereas trophoblasts markedly decrease their proliferation during the transition from development to maturation in the normal placenta (Fig. S9). We identified G9a as a key regulator required for coordinated proliferation of endothelial and trophoblast cells, and labyrinth expansion. Inactivation of G9a in endothelial progenitors and their derivatives caused a decrease in endothelial proliferation with a concomitant increase in trophoblast proliferation and decreased labyrinth expansion. Furthermore, deficiency of G9a results in decreased expression of Notch pathway effectors (Fig. S9), and activation of the Notch pathway rescues labyrinth expansion. This study describes the first mouse model of deficient placental vascular maturation and provides insight into the regulatory pathways.

It has been proposed that a reduction in trophoblast proliferation during placental maturation is required for vascular elongation driven by endothelial cell proliferation, and that the balance between VEGFA (a member of the vascular endothelial growth factor family) and placental growth factor (PlGF; also known as PGF), which are secreted by both endothelial cells and the trophoblast (Barker et al., 2010), is involved. In contrast to VEGFA, PlGF, a regulator of trophoblast differentiation (Maglione et al., 1993), suppresses angiogenesis. Therefore, paracrine signaling between the endothelium and the trophoblast might regulate placental vasculature maturation. We found that deletion of *G9a* in endothelial progenitors causes a decrease in proliferation of endothelial cells and increased proliferation of the trophoblast. This indicates that G9a is required in the labyrinth to limit trophoblast expansion. However, neither *Plgf* nor *Vegfa* was misregulated in *G9a* mutant placentae, suggesting that alternative molecules might mediate communication from the endothelium to limit trophoblast proliferation. Our RNAseq data revealed that the *G9a* mutant labyrinth overexpresses secreted protein-encoding genes, including secreted modular calcium-binding protein 1 (Smoc1) and arylsulfatase family member 1 (Arsi). Smoc1 is expressed in endothelial cells and positively regulates cell proliferation (Awwad et al., 2015), and Arsi is secreted from proliferating long-term self-renewing neuroepithelial-like stem cells (Doerr et al., 2015). Thus, placental endothelial cells might limit trophoblast proliferation via G9a-mediated repression of secreted activators of cell proliferation.

Activating the Notch pathway in *G9a* mutant placental endothelial progenitors rescued placental endothelial cell proliferation and labyrinth expansion (Fig. 6). This suggests that the Notch pathway stimulates endothelial cell proliferation in the placenta. Notch signaling has been shown to both repress and promote endothelial cell proliferation in different systems. Dll4/Notch signaling restricts angiogenesis to tip cells, which guide new sprouts, and inhibits angiogenic responses in other endothelial cells (Siekmann and Lawson, 2007). Accordingly, Notch deficiency leads to excessive proliferation of endothelial cells in segmental arteries in zebrafish (Leslie et al., 2007). In contrast, the Notch ligand jagged 1 promotes angiogenesis by antagonizing Dll4/Notch signaling in mouse retinal endothelium (Ehling et al., 2013). In addition, inhibition of Dll4/Notch signaling increases sprouting and density of nonfunctional blood vessels (Noguera-Troise et al., 2006; Ridgway et al., 2006). Our finding that Notch effectors are downregulated in *G9a*-mutant labyrinth endothelium and in the chorionic villi of human placentae affected by IUGR opens the possibility that pharmacological activation of the Notch pathway in the placenta might be a potential strategy to prevent or treat abnormal maturation of the placental vasculature. Valproic acid, which is used to control epileptic seizures and psychiatric disorders, was

Development (2017) 144, 1976-1987 doi:10.1242/dev.148916

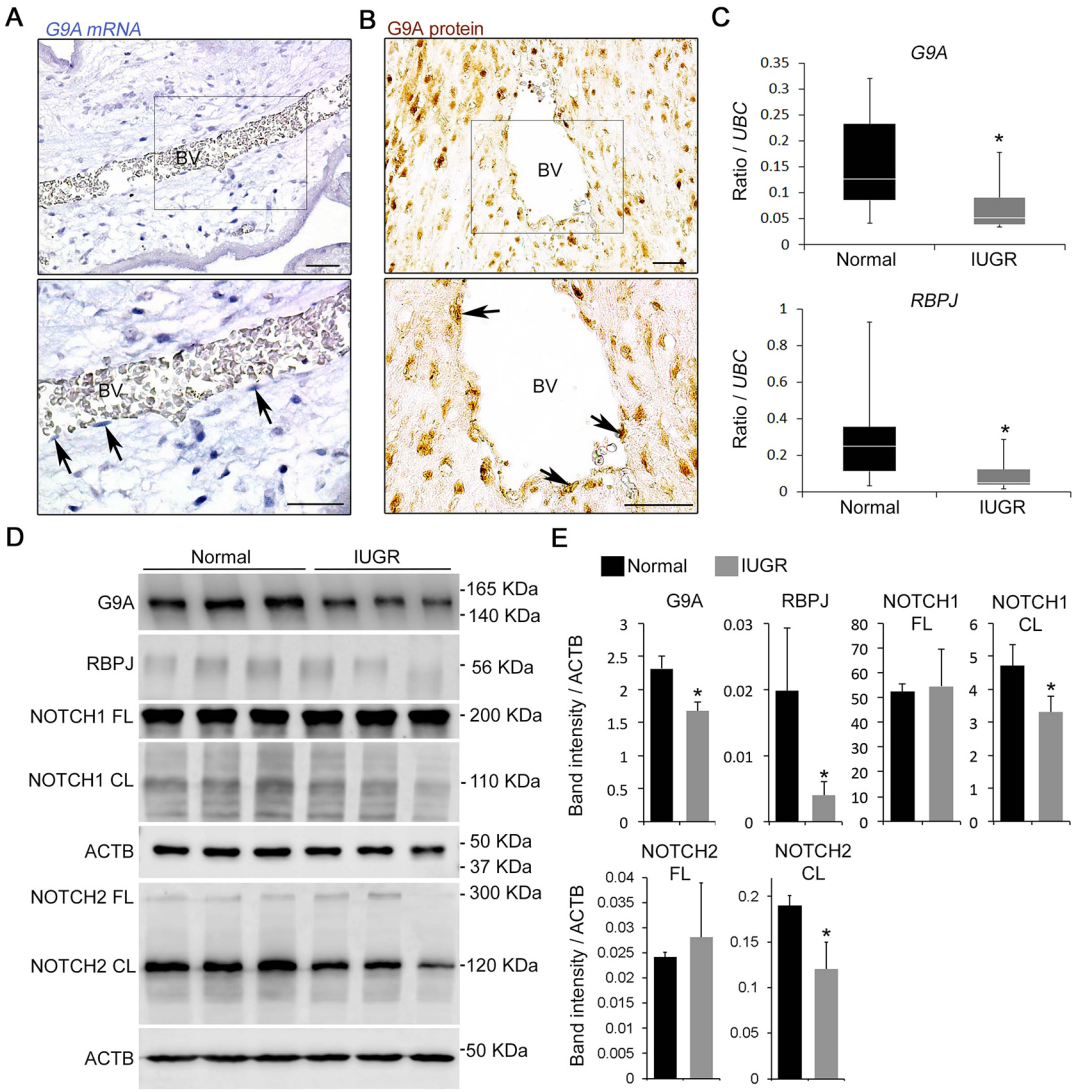

Fig. 7. G9A and RBPJ are downregulated in placentae affected by IUGR. (A,B) *In situ* hybridization (A) and immunohistochemistry (B) for G9A in normal human placentae. Arrows point to endothelial cells in blood vessels (BV). Lower panels show higher magnification of the boxed areas in upper panels. Scale bars: 50 µm. (C) qPCR for *G9A* and *RBPJ* in placenta from normal and IUGR pregnancies between 26 and 37 weeks. Data are presented as the ratio over ubiquitin C (*UBC*) and represent the mean±s.d. of ten placentae per group. **P*<0.05. (D) Western blot for G9A, RBPJ, full length (FL) and cleaved (CL) NOTCH1 and NOTCH2, and β-actin (ACTB), used as loading control, on protein lysates from placentae from normal and IUGR pregnancies. Blots are representative of six samples analyzed per condition. (E) Quantification of band intensity relative to ACTB of the blots shown in D. Data represent the mean±s.d. of six placentae per condition. **P*<0.05.

found to activate the Notch pathway resulting in increased activity of Rbpj (Pinchot et al., 2011). The use of valproic acid during pregnancy has limitations as it can promote a higher risk of neural tube closure defects in babies when administered during the first trimester of pregnancy (Jentink et al., 2010). However, the transition from development to maturation occurs in the second trimester (fifth month of pregnancy) (Benirschke et al., 2012). Therefore, valproic acid treatment after the first trimester could be tested as a way to prevent or correct abnormal maturation of the placental vasculature. Our mouse model will be useful for testing the capacity of valproic acid to activate the Notch pathway in placental endothelium and its effect on placental endothelial cell and trophoblast proliferation and vascular maturation.

IUGR is diagnosed by ultrasound only when the placenta is malfunctioning (Albaiges et al., 2000) or the fetus is smaller than expected for the gestational age (Yoshida et al., 2000). Uncovering the cellular and molecular events dysregulated in the developing placenta that affect vascular maturation and precede clinical manifestation is required to develop methods to identify fetuses at risk of IUGR or other abnormalities associated with placental insufficiency. We found that deficiency of G9a in placental endothelial cells alters placental morphology starting at E13.5. Importantly, we found that the decreased ratio of endothelial cell and spongiotrophoblast proliferation at E11.5 precedes morphological defects in the labyrinth and spongiotrophoblast, which were first detected at E12.5 (Figs 1 and 4). Therefore, it is possible that an altered ratio of endothelial cells versus trophoblast proliferation is an early manifestation of placental maturation defects. Our mouse model will be useful to identify molecules associated with an abnormal endothelial cell/spongiotrophoblast proliferation ratio that could be investigated as potential biomarkers of placental maturation defects.

Development (2017) 144, 1976-1987 doi:10.1242/dev.148916

MATERIALS AND METHODS

Mice

Mouse lines: *G9a*$^{fl/fl}$ (Sampath et al., 2007), *Tie2-Cre* (Proctor et al., 2005), *Rosa*$^{mT/mG}$ (Muzumdar et al., 2007) and *Rosa*^{Notch} (Murtaugh et al., 2003). Procedures followed the Canadian Council for Animal Care guidelines, and were approved by the Animal Care Committee at The Centre for Phenogenomics. Embryos and placentae were dissected in cold PBS and fixed in 4% paraformaldehyde for 2 h at 4°C, dehydrated in an ethanol series and stored at −20°C until processing. Embryos and placentae were rehydrated by reversing the ethanol series before processing. Littermates from at least two litters were analyzed.

Transmission electron microscopy (TEM)

Samples were fixed in 2% glutaraldehyde in 0.1 M sodium cacodylate buffer, rinsed in buffer, post-fixed in 1% osmium tetroxide in buffer, dehydrated in a graded ethanol series followed by propylene oxide, and embedded in Quetol-Spurr resin. Sections (90 nm thick) were cut on a Leica Ultracut ultramicrotome, stained with uranyl acetate and lead citrate and viewed in an FEI Tecnai 20 transmission electron microscope.

Injection of contrast agent and microCT scanning of fetoplacental vasculature

Detailed methods for microCT imaging have been described (Rennie et al., 2015, 2014; Whiteley et al., 2006). Briefly, uteri were dissected at E15.5 and immersed in ice-cold PBS. Each fetus was dissected from the uterus while maintaining the vascular connection to the placenta. Embryos were immersed in warm PBS to resume blood circulation. A catheter was inserted into the umbilical artery and the fetus was perfused with saline (with heparin, 100 units/ml) followed by radio-opaque silicone rubber contrast agent (Microfil; Flow Technology). Following perfusion, specimens were fixed (10% formalin) for 24-48 h at 4°C. Specimens were scanned using a Bruker SkyScan1172 high-resolution microCT scanner at a resolution of 7.1 µm and 996 views were acquired via 180-degree rotation with an X-ray source at 54 kVp and 185 µA. Three-dimensional data were reconstructed using SkyScan NRecon software.

Vessel segmentation and statistical analysis

The structure of the vasculature was identified automatically using a segmentation algorithm (Rennie et al., 2011). The leaves of the vascular tree were pruned to 35 µm for data consistency. Analysis was performed on seven controls and four mutants. Each group contains a minimum of three dams and two to three specimens per litter. The span and depth of the fetoplacental arterial tree were measured from the surface renderings via digital calipers using the Amira software package (Visage Imaging). To quantify vessel curvature, a tortuosity ratio was computed (Rennie et al., 2011) by determining the ratio of the vascular path length to the Euclidian (i.e. beeline) distance from the umbilical artery to each terminal vessel. The number of branching generations in each specimen was determined using a Strahler ordering scheme (Rennie et al., 2015), which numbers vessels in an upstream direction starting from the terminal vessel segments. The geometric and morphological features of the vascular trees were analyzed using *t*-tests. A two-way ANOVA determined whether there was an effect of group on the average diameter of the Strahler order vessels, followed by *t*-tests to compare mutants with controls at each Strahler order number. A value of $P<0.05$ was considered significant.

RNAseq and computational analysis

RNA was isolated from the dissected labyrinth of control *G9a*$^{fl/fl}$ and mutant *G9a*$^{fl/fl}$;Tie2-cre placentae at E12.5 and E13.5 using the Direct-zol RNA MiniPrep Plus Kit (Zymo Research). mRNA was pulled down using the NEBNext Poly(A) mRNA magnetic isolation module (New England Biolabs). RNAseq libraries were prepared using the NEBNext Ultra Directional RNA Library Prep Kit (New England Biolabs), and sequenced on the Illumina HiSeq 2500 platform. Sequencing reads were trimmed using Trimmomatic (Bolger et al., 2014) and mapped to the mouse genome (mm10) using STAR (Dobin et al., 2013). Mapped read counts were obtained using HTseq (Anders et al., 2015). Differential expression analysis was performed using DESeq2 (Love et al., 2014). Clustering was performed using Cluster 3.0 and visualized with Treeview (Saldanha, 2004). Enrichment of gene ontology categories was determined using DAVID (Huang et al., 2009). GSEA pre-ranked enrichment analysis with GSEA v2.2.0 (GSEA) (Subramanian et al., 2005) identified pathways associated with genes misregulated in *G9a* mutant placental endothelial cells. Transcripts were ranked according to fold change. Analysis involved 1000 random permutations using the 'h.all.v5.1.symbols.gmt' Hallmarks gene set. Gene sets with more than 125 or fewer than ten genes were excluded from the analysis. RNAseq data were deposited in Gene Expression Omnibus with entry GSE97579.

In situ hybridization

Sections (7 µm thick) were obtained from placental samples embedded in paraffin and processed as described previously (Chi and Delgado-Olguin, 2013).

qPCR

GFP^{+} endothelial cells were sorted from control (*G9a*$^{fl/+}$;*Tie2-Cre*;*Rosa*$^{mT/mG}$) and *G9a* mutant (*G9a*$^{fl/fl}$;*Tie2-Cre*;*Rosa*$^{mT/mG}$) labyrinth at E12.5 and E13.5. cDNA was synthesized from 10 ng of total RNA using the SuperScript VILO cDNA Synthesis Kit (Thermo Fisher Scientific). For qPCR, 10 pg of cDNA were used with SsoAdvanced Universal SYBR Green Supermix (Bio-Rad). qPCR was performed using a CFX384 Touch Real-Time PCR Detection System (Bio-Rad) using the primers listed in Table S3.

Immunofluorescence

Sections were stained as previously described (Delgado-Olguin et al., 2014). Primary antibodies and dilutions were: G9a (Cell Signaling Technology, 3306, 1/200), H3K9me2 (Cell Signaling Technology, 9753, 1/500), GFP (GeneScript, A01694, 1/1000), Pecam1/CD34 (BD Pharmingen, 553370, 1/200), phosphorylated histone H3 (Abcam, AB5176, 1/200), activated caspase 3 (Sigma, C8487, 1/200), trophoblast specific protein alpha (Abcam, ab104401, 1/50), ZO1 (Thermo Fisher Scientific, 61-7300, 1/100), pHH3 (Santa Cruz, SC-8656-R, 1/200), Notch1 (bTAN 20, 1/200) and Notch2 (C651.6DbHN, 1/200) (Developmental Studies Hybridoma Bank). Secondary antibodies were goat anti-rabbit Alexa Fluor 568 (A-11011), goat anti-chicken Alexa Fluor 488 (A-11039), donkey anti-rat Alexa Fluor 488 (A-21208) and goat anti-mouse Alexa Fluor 568 (A-11004). (Thermo Fisher Scientific, 1/700). DAPI (Sigma, D9564, 1/1000) was used for nuclear staining.

Endothelial cell sorting and culture

GFP^{+} endothelial cells were sorted from control *G9a*$^{fl/+}$;*Tie2-Cre*;*Rosa*$^{mT/mG}$ and mutant *G9a*$^{fl/fl}$;*Tie2-Cre*;*Rosa*$^{mT/mG}$ placentae at E13.5. Placentae were disassociated in TrypLE Express (Thermo Fisher Scientific, 12604-013) at 37°C for 30 min. After centrifugation, pellets were incubated in 1× Red Blood Cell Lysis Solution (MACS Miltenyi Biotec, 130-094-183) at room temperature for 10 min. Cells were diluted with 250 µl of DMEM (Wisent, 319-005-CL) containing 1% fetal bovine serum, 1 mM EDTA and 2 µg/ml propidium iodide (Sigma, P4170) for detection of dead cells. Cells were sorted using MoFlo-Astrios BYRV equipment then 10,000 cells were seeded on 96-well plates coated with 0.1% gelatin and cultured for 3 days in endothelial cell medium containing Endothelial Cell Growth Supplement (ECGS; Sigma, E2759), 10% fetal bovine serum and 100 ng/ml of human VEGF (R&D Systems, 293-VE-010). Cultured endothelial cell length was measured on micrographs using ImageJ.

Human placenta samples

The Biobank at Mount Sinai Hospital, and the Sant'Anna Hospital, University of Turin, Italy collected tissues from elective pregnancy terminations after informed consent. Specimen collection followed ethics guidelines of the University of Toronto, the Research Ethics Board of Mount Sinai Hospital, and the World Medical Association Declaration of Helsinki. Ten placentae from singleton normal and ten from intrauterine growth restriction (IUGR) pregnancies were obtained. IUGR placentae were selected according to the American College of Obstetricians and

Development (2017) 144, 1976-1987 doi:10.1242/dev.148916

Gynaecologists guidelines (American College of Obstetricians and Gynecologists, 2013). Participants were healthy women without signs of hypertension, pre-eclampsia, or known causes of IUGR including renal, endocrine and autoimmune disorders. IUGR cases included exhibited abnormal umbilical artery Doppler defined as absence or reverse of end diastolic velocity and a birth weight below the fifth percentile for gestational age. Normotensive age-matched preterm controls were selected based on the absence of placental disease with appropriate-for-gestational-age fetuses. Tissues were collected from pregnancies that did not exhibit any fetal and chromosomal abnormalities. Maternal characteristics are shown in Table S4.

Acknowledgements

We thank Alexander Tarakhovsky (The Rockefeller University) for the *G9a* floxed line; Tullia Trodros (University of Turin) for placental samples; Doug Holmyard (Advanced Bioimaging Centre, Mount Sinai Hospital and The Hospital for Sick Children) for TEM; Lisa X. Yu (SickKids Mouse Imaging Centre) for micro-CT; Andrea Tagliaferro (Mount Sinai Hospital) for obtaining human samples; Rong Mo (Chi-chung Hui's Lab, The Hospital for Sick Children) for sectioning and staining; Sheyun Zhao (SickKids-UHN Flow Cytometry Facility) for cell sorting; Paul Paroutis (Imaging Facility at The Hospital for Sick Children) for help with confocal microscopy; Sergio Pereira (The Centre for Applied Genomics) for next generation sequencing; TCP (The Centre for Phenogenomics) for mouse husbandry and care; Jason Fish (University Health Network) for advice and critical reading of the manuscript; Koroboshka Brand-Arzamendi for graphics in Fig. S9; and Natalia Kaniuk (Grant Development Office, The Hospital for Sick Children) for editorial assistance.

Competing interests

The authors declare no competing or financial interests.

Author contributions

Conceptualization: L. Chi, P.D.; Methodology: L. Chi, A.A., L.S.C., P.D.; Validation: L. Chi, A.R.R.; Formal analysis: L. Chi, P.D.; Investigation: L. Chi, A.A., A.R.R., S.V., L.S.C., L. Caporiccio, J.G.S., M.D.W.; Resources: M.D.W.; Data curation: J.G.S., I.C.; Writing - original draft: P.D.; Writing - review & editing: L. Chi, A.A., A.R.R., S.V., L.S.C., L. Caporiccio, J.G.S., I.C., M.D.W., P.D.-O.; Visualization: P.D.-O.; Supervision: P.D.-O.; Project administration: P.D.-O.; Funding acquisition: P.D.-O.

Funding

This work was funded by the Heart and Stroke Foundation of Canada (G-17-0018613), Operational Funds from the Hospital for Sick Children (to P.D.-O.), the Natural Sciences and Engineering Research Council of Canada (NSERC) (500865 to P.D.-O.; 436194-2013 to M.D.W.) and the Canadian Institutes of Health Research (CIHR) (PJT-149046 to P.D.-O.; MOP-133436 to I.C.; MOP130403 to J.G.S.). M.D.W. is the Canada Research Chair (Tier 2) in Comparative Genomics.

Data availability

RNAseq data have been deposited in Gene Expression Omnibus under accession number GSE97579 (https://www.ncbi.nlm.nih.gov/geo/query/acc.cgi?acc=GSE97579).

Supplementary information

Supplementary information available online at http://dev.biologists.org/lookup/doi/10.1242/dev.148916.supplemental

References

Adamson, S. L., Lu, Y., Whiteley, K. J., Holmyard, D., Hemberger, M., Pfarrer, C. and Cross, J. C. (2002). Interactions between trophoblast cells and the maternal and fetal circulation in the mouse placenta. *Dev. Biol.* **250**, 358-373.

Albaiges, G., Missfelder-Lobos, H., Lees, C., Parra, M. and Nicolaides, K. H. (2000). One-stage screening for pregnancy complications by color Doppler assessment of the uterine arteries at 23 weeks' gestation. *Obstet. Gynecol.* **96**, 559-564.

American College of Obstetricians and Gynecologists. (2013). ACOG Practice bulletin no. 134: fetal growth restriction. *Obstet. Gynecol.* **121**, 1122-1133.

Ananth, C. V. and Vintzileos, A. M. (2009). Distinguishing pathological from constitutional small for gestational age births in population-based studies. *Early Hum. Dev.* **85**, 653-658.

Anders, S., Pyl, P. T. and Huber, W. (2015). HTSeq–a Python framework to work with high-throughput sequencing data. *Bioinformatics* **31**, 166-169.

Awwad, K., Hu, J., Shi, L., Mangels, N., Abdel Malik, R., Zippel, N., Fisslthaler, B., Eble, J. A., Pfeilschifter, J., Popp, R. et al. (2015). Role of secreted modular calcium-binding protein 1 (SMOC1) in transforming growth factor beta signalling and angiogenesis. *Cardiovasc. Res.* **106**, 284-294.

Barker, D. J., Osmond, C., Golding, J., Kuh, D. and Wadsworth, M. E. (1989). Growth in utero, blood pressure in childhood and adult life, and mortality from cardiovascular disease. *BMJ* **298**, 564-567.

Barker, D. J. P., Thornburg, K. L., Osmond, C., Kajantie, E. and Eriksson, J. G. (2010). The surface area of the placenta and hypertension in the offspring in later life. *Int. J. Dev. Biol.* **54**, 525-530.

Barut, F., Barut, A., Gun, B. D., Kandemir, N. O., Harma, M. I., Harma, M., Aktunc, E. and Ozdamar, S. O. (2010). Intrauterine growth restriction and placental angiogenesis. *Diagn. Pathol.* **5**, 24.

Benirschke, K., Burton, G. J. and Baergen, N. R. (2012). Architecture of normal villous trees. In *Pathology of the Human Placenta*, pp. 101-144: Springer-Verlag.

Bolger, A. M., Lohse, M. and Usadel, B. (2014). Trimmomatic: a flexible trimmer for Illumina sequence data. *Bioinformatics* **30**, 2114-2120.

Chi, L. and Delgado-Olguin, P. (2013). Expression of NOL1/NOP2/sun domain (Nsun) RNA methyltransferase family genes in early mouse embryogenesis. *Gene Expr. Patterns* **13**, 319-327.

Copeland, J. N., Feng, Y., Neradugomma, N. K., Fields, P. E. and Vivian, J. L. (2011). Notch signaling regulates remodeling and vessel diameter in the extraembryonic yolk sac. *BMC Dev. Biol.* **11**, 12.

Delgado-Olguin, P., Dang, L. T., He, D., Thomas, S., Chi, L., Sukonnik, T., Khyzha, N., Dobenecker, M.-W., Fish, J. E. and Bruneau, B. G. (2014). Ezh2-mediated repression of a transcriptional pathway upstream of Mmp9 maintains integrity of the developing vasculature. *Development* **141**, 4610-4617.

Demicheva, E. and Crispi, F. (2014). Long-term follow-up of intrauterine growth restriction: cardiovascular disorders. *Fetal Diagn. Ther.* **36**, 143-153.

Dobin, A., Davis, C. A., Schlesinger, F., Drenkow, J., Zaleski, C., Jha, S., Batut, P., Chaisson, M. and Gingeras, T. R. (2013). STAR: ultrafast universal RNA-seq aligner. *Bioinformatics* **29**, 15-21.

Doerr, J., Böckenhoff, A., Ewald, B., Ladewig, J., Eckhardt, M., Gieselmann, V., Matzner, U., Brüstle, O. and Koch, P. (2015). Arylsulfatase A overexpressing human iPSC-derived neural cells reduce CNS sulfatide storage in a mouse model of metachromatic leukodystrophy. *Mol. Ther.* **23**, 1519-1531.

Ehling, M., Adams, S., Benedito, R. and Adams, R. H. (2013). Notch controls retinal blood vessel maturation and quiescence. *Development* **140**, 3051-3061.

Galasso, G., Schiekofer, S., Sato, K., Shibata, R., Handy, D. E., Ouchi, N., Leopold, J. A., Loscalzo, J. and Walsh, K. (2006). Impaired angiogenesis in glutathione peroxidase-1-deficient mice is associated with endothelial progenitor cell dysfunction. *Circ. Res.* **98**, 254-261.

Griffin, C. T., Curtis, C. D., Davis, R. B., Muthukumar, V. and Magnuson, T. (2011). The chromatin-remodeling enzyme BRG1 modulates vascular Wnt signaling at two levels. *Proc. Natl. Acad. Sci. USA* **108**, 2282-2287.

Huang, D. W., Sherman, B. T. and Lempicki, R. A. (2009). Systematic and integrative analysis of large gene lists using DAVID bioinformatics resources. *Nat. Protoc.* **4**, 44-57.

Inagawa, M., Nakajima, K., Makino, T., Ogawa, S., Kojima, M., Ito, S., Ikenishi, A., Hayashi, T., Schwartz, R. J., Nakamura, K. et al. (2013). Histone H3 lysine 9 methyltransferases, G9a and GLP are essential for cardiac morphogenesis. *Mech. Dev.* **130**, 519-531.

Jentink, J., Loane, M. A., Dolk, H., Barisic, I., Garne, E., Morris, J. K. and de Jong-van den Berg, L. T. W. (2010). Valproic acid monotherapy in pregnancy and major congenital malformations. *N. Engl. J. Med.* **362**, 2185-2193.

Kaufmann, P., Bruns, U., Leiser, R., Luckhardt, M. and Winterhager, E. (1985). The fetal vascularisation of term human placental villi. II. Intermediate and terminal villi. *Anat. Embryol.* **173**, 203-214.

Knox, K. and Baker, J. C. (2008). Genomic evolution of the placenta using co-option and duplication and divergence. *Genome Res.* **18**, 695-705.

Kuleshov, M. V., Jones, M. R., Rouillard, A. D., Fernandez, N. F., Duan, Q., Wang, Z., Koplev, S., Jenkins, S. L., Jagodnik, K. M., Lachmann, A. et al. (2016). Enrichr: a comprehensive gene set enrichment analysis web server 2016 update. *Nucleic Acids Res.* **44**, W90-W97.

Lammert, E., Cleaver, O. and Melton, D. (2003). Role of endothelial cells in early pancreas and liver development. *Mech. Dev.* **120**, 59-64.

Lazrak, M., Deleuze, V., Noel, D., Haouzi, D., Chalhoub, E., Dohet, C., Robbins, I. and Mathieu, D. (2004). The bHLH TAL-1/SCL regulates endothelial cell migration and morphogenesis. *J. Cell Sci.* **117**, 1161-1171.

Leslie, J. D., Ariza-McNaughton, L., Bermange, A. L., McAdow, R., Johnson, S. L. and Lewis, J. (2007). Endothelial signalling by the Notch ligand Delta-like 4 restricts angiogenesis. *Development* **134**, 839-844.

Love, M. I., Huber, W. and Anders, S. (2014). Moderated estimation of fold change and dispersion for RNA-seq data with DESeq2. *Genome Biol.* **15**, 550.

Maglione, D., Guerriero, V., Viglietto, G., Ferraro, M. G., Aprelikova, O., Alitalo, K., Del Vecchio, S., Lei, K. J., Chou, J. Y. and Persico, M. G. (1993). Two alternative mRNAs coding for the angiogenic factor, placenta growth factor (PlGF), are transcribed from a single gene of chromosome 14. *Oncogene* **8**, 925-931.

Murtaugh, L. C., Stanger, B. Z., Kwan, K. M. and Melton, D. A. (2003). Notch signaling controls multiple steps of pancreatic differentiation. *Proc. Natl. Acad. Sci. USA* **100**, 14920-14925.

Muzumdar, M. D., Tasic, B., Miyamichi, K., Li, L. and Luo, L. (2007). A global double-fluorescent Cre reporter mouse. *Genesis* **45**, 593-605.

Nagano, T., Mitchell, J. A., Sanz, L. A., Pauler, F. M., Ferguson-Smith, A. C., Feil, R. and Fraser, P. (2008). The Air noncoding RNA epigenetically silences transcription by targeting G9a to chromatin. *Science* **322**, 1717-1720.

Noguera-Troise, I., Daly, C., Papadopoulos, N. J., Coetzee, S., Boland, P., Gale, N. W., Lin, H. C., Yancopoulos, G. D. and Thurston, G. (2006). Blockade of Dll4 inhibits tumour growth by promoting non-productive angiogenesis. *Nature* **444**, 1032-1037.

Oh, S.-T., Kim, K.-B., Chae, Y.-C., Kang, J.-Y., Hahn, Y. and Seo, S.-B. (2014). H3K9 histone methyltransferase G9a-mediated transcriptional activation of p21. *FEBS Lett.* **588**, 685-691.

Pedrosa, A.-R., Trindade, A., Fernandes, A.-C., Carvalho, C., Gigante, J., Tavares, A. T., Dieguez-Hurtado, R., Yagita, H., Adams, R. H. and Duarte, A. (2015). Endothelial Jagged1 antagonizes Dll4 regulation of endothelial branching and promotes vascular maturation downstream of Dll4/Notch1. *Arterioscler. Thromb. Vasc. Biol.* **35**, 1134-1146.

Pinchot, S. N., Jaskula-Sztul, R., Ning, L., Peters, N. R., Cook, M. R., Kunnimalaiyaan, M. and Chen, H. (2011). Identification and validation of Notch pathway activating compounds through a novel high-throughput screening method. *Cancer* **117**, 1386-1398.

Proctor, J. M., Zang, K., Wang, D., Wang, R. and Reichardt, L. F. (2005). Vascular development of the brain requires beta8 integrin expression in the neuroepithelium. *J. Neurosci.* **25**, 9940-9948.

Purcell, D. J., Jeong, K. W., Bittencourt, D., Gerke, D. S. and Stallcup, M. R. (2011). A distinct mechanism for coactivator versus corepressor function by histone methyltransferase G9a in transcriptional regulation. *J. Biol. Chem.* **286**, 41963-41971.

Rennie, M. Y., Detmar, J., Whiteley, K. J., Yang, J., Jurisicova, A., Adamson, S. L. and Sled, J. G. (2011). Vessel tortuousity and reduced vascularization in the fetoplacental arterial tree after maternal exposure to polycyclic aromatic hydrocarbons. *Am. J. Physiol. Heart Circ. Physiol.* **300**, H675-H684.

Rennie, M. Y., Whiteley, K. J., Sled, J. G. and Adamson, S. L. (2014). Scanning electron microscopy and micro-computed tomography imaging of the utero- and fetoplacental circulations. In *The Guide to Investigation of Mouse Pregnancy* (ed. A. Croy, A. T. Yamada, F. J. DeMayo & S. L. Adamson), pp. 637-648. USA: Academic Press.

Rennie, M. Y., Rahman, A., Whiteley, K. J., Sled, J. G. and Adamson, S. L. (2015). Site-specific increases in utero- and fetoplacental arterial vascular resistance in eNOS-deficient mice due to impaired arterial enlargement. *Biol. Reprod.* **92**, 48.

Ridgway, J., Zhang, G., Wu, Y., Stawicki, S., Liang, W.-C., Chanthery, Y., Kowalski, J., Watts, R. J., Callahan, C., Kasman, I. et al. (2006). Inhibition of Dll4 signalling inhibits tumour growth by deregulating angiogenesis. *Nature* **444**, 1083-1087.

Roca, C. and Adams, R. H. (2007). Regulation of vascular morphogenesis by Notch signaling. *Genes Dev.* **21**, 2511-2524.

Sahin, Z., Acar, N., Ozbey, O., Ustunel, I. and Demir, R. (2011). Distribution of Notch family proteins in intrauterine growth restriction and hypertension complicated human term placentas. *Acta Histochem.* **113**, 270-276.

Saldanha, A. J. (2004). Java Treeview–extensible visualization of microarray data. *Bioinformatics* **20**, 3246-3248.

Sampath, S. C., Marazzi, I., Yap, K. L., Sampath, S. C., Krutchinsky, A. N., Mecklenbräuker, I., Viale, A., Rudensky, E., Zhou, M.-M., Chait, B. T. et al. (2007). Methylation of a histone mimic within the histone methyltransferase G9a regulates protein complex assembly. *Mol. Cell* **27**, 596-608.

Secchiero, P., Corallini, F., Gonelli, A., Dell'Eva, R., Vitale, M., Capitani, S., Albini, A. and Zauli, G. (2007). Antiangiogenic activity of the MDM2 antagonist nutlin-3. *Circ. Res.* **100**, 61-69.

Shaut, C. A. E., Keene, D. R., Sorensen, L. K., Li, D. Y. and Stadler, H. S. (2008). HOXA13 is essential for placental vascular patterning and labyrinth endothelial specification. *PLoS Genet.* **4**, e1000073.

Shinkai, Y. and Tachibana, M. (2011). H3K9 methyltransferase G9a and the related molecule GLP. *Genes Dev.* **25**, 781-788.

Siekmann, A. F. and Lawson, N. D. (2007). Notch signalling limits angiogenic cell behaviour in developing zebrafish arteries. *Nature* **445**, 781-784.

Subramanian, A., Tamayo, P., Mootha, V. K., Mukherjee, S., Ebert, B. L., Gillette, M. A., Paulovich, A., Pomeroy, S. L., Golub, T. R., Lander, E. S. et al. (2005). Gene set enrichment analysis: a knowledge-based approach for interpreting genome-wide expression profiles. *Proc. Natl. Acad. Sci. USA* **102**, 15545-15550.

Tachibana, M., Sugimoto, K., Nozaki, M., Ueda, J., Ohta, T., Ohki, M., Fukuda, M., Takeda, N., Niida, H., Kato, H. et al. (2002). G9a histone methyltransferase plays a dominant role in euchromatic histone H3 lysine 9 methylation and is essential for early embryogenesis. *Genes Dev.* **16**, 1779-1791.

Ubezio, B., Blanco, R. A., Geudens, I., Stanchi, F., Mathivet, T., Jones, M. L., Ragab, A., Bentley, K. and Gerhardt, H. (2016). Synchronization of endothelial Dll4-Notch dynamics switch blood vessels from branching to expansion. *Elife* **5**, e12167.

Versaevel, M., Grevesse, T. and Gabriele, S. (2012). Spatial coordination between cell and nuclear shape within micropatterned endothelial cells. *Nat. Commun.* **3**, 671.

Wagschal, A., Sutherland, H. G., Woodfine, K., Henckel, A., Chebli, K., Schulz, R., Oakey, R. J., Bickmore, W. A. and Feil, R. (2008). G9a histone methyltransferase contributes to imprinting in the mouse placenta. *Mol. Cell. Biol.* **28**, 1104-1113.

Whiteley, K. J., Pfarrer, C. D. and Adamson, S. L. (2006). Vascular corrosion casting of the uteroplacental and fetoplacental vasculature in mice. *Methods Mol. Med.* **121**, 371-392.

Yoshida, S., Unno, N., Kagawa, H., Shinozuka, N., Kozuma, S. and Taketani, Y. (2000). Prenatal detection of a high-risk group for intrauterine growth restriction based on sonographic fetal biometry. *Int. J. Gynaecol. Obstet.* **68**, 225-232.